# Pair weakening and tunnel channels at cuprate interfaces

J. Halbritter
*Kernforschungszentrum Karlsruhe, Institut für Materialforschung I, Postfach 3640, 7500 Karlsruhe 1, Germany*
(Received 2 March 1992; revised manuscript received 27 August 1992)

The very high superconducting transition temperatures $T_c$ of cuprates are not yet substantiated in applications which seem intimately related to the layered nature of the cuprous oxides. Based on a highly directional *p-d* hybridization and correlation, the layering causes a correlated quasi-two-dimensional conduction in the $CuO_2$ planes. The basis for the superconductivity seems to be the low carrier density ($n_s \geq 10^{21}/\mathrm{cm}^3\,\mathrm{eV}$) close to the metal-insulator transition (MIT) in two dimensions. Thus, any perturbation degrading hybridization and correlation renders the cuprate insulating, which then by disorder contains localized states ($n_L \leq 10^{21}/\mathrm{cm}^3$). In this layered material the correlated conduction is only weakly hindered by point defects. More prominent perturbations for the conduction are external or internal surfaces with reduced hybridization by a reduced dimensionality and by disorder in energy, distance, or bond angle which occurs intrinsically by relaxation of dangling bonds. This intrinsic, insulating seam with its localized states weakens superconductivity and supports tunneling in various channels. The weakening by on-site Coulomb repulsion close to the MIT smears out and roughens the metal-insulator interface and, e.g., causes reduced and locally varying energy gaps and leakage current $j_{bl}$. The different tunnel channels—direct and resonant or intermediate via localized states $n_L$—have different distance $d$, temperature $T$, and voltage $U$ dependencies. This explains not only the observed $I(d,T,U)$ dependencies in scanning-tunneling microscopy, break, or broad area junctions, but also the background conduction and the degradation of Josephson currents $j_c(T,H)$ across weak links is explained together with the $j_c R_{bn} \propto 1/R_{bn}^m$ $(1 \leq m \leq 1.5)$ dependence on grain boundary resistance $R_{bn}$; the leakage current $j_{bl} \propto 1/R_{bn}$ and their noise $\propto j_{bl}$; and the rf residual losses $R_{\mathrm{res}} \propto R_{bn}^2$. The proposed intermediate-state tunnel model fits all *a-b* plane weak links and serves as a microscopic base for mean-field (proximity effect) descriptions for the intrinsic degradation of superconductivity at interfaces. The intermediate-state tunneling is correlated yielding the Coulomb barrier by localization; Cooper pair tunneling, e.g., by negative $U$ centers; and other many particle effects.

## I. INTRODUCTION

Whereas the structure and composition of bulk cuprate superconductors are fairly well established,[1,2] little is known on the nature of external and internal surfaces.[3,4] In addition, most surface studies concentrate on the "dead," i.e., insulating $\hat{c}$-axis surface and not on the more relevant intrinsic or extrinsic $\hat{a}$-$\hat{b}$ surfaces—see Fig. 1 or Sec. II. Less is known on microscopic conduction mechanism and superconducting interaction in the bulk.[5,6] Least is known on conduction mechanisms across surfaces and interfaces. Proposals for conduction across surfaces and interfaces reach from normal conducting layers and proximity effect[7] to pair breaking by spin-flip scattering[8] or pair weakening by localized states.[3] The latter is elaborated in Sec. II and compared successfully with experiments in Sec. III.

The analysis of the conduction across surfaces and interfaces is the goal of this paper, where we use $YBa_2Cu_2O_x$ (YBCO) as a model. For doing so, five central facts should be noted. *First,* the existence of "normal conduction" has only been inferred by many researchers from the degraded critical currents observed in the superconducting state. The necessary ($>10$ nm) "normal material" associated with these weak links (WL) has never been identified directly. *Second,* no normal (metallic) conducting phase has been found in the phase diagram of YBCO.[1,2] *Third,* no impurity phase has been found at weak links.[3,4] *Fourth,* disorder in distance, direction, or energy (e.g., due to strain or O disorder or surfaces) in the $CuO_2$ planes change the delicate hybridization between

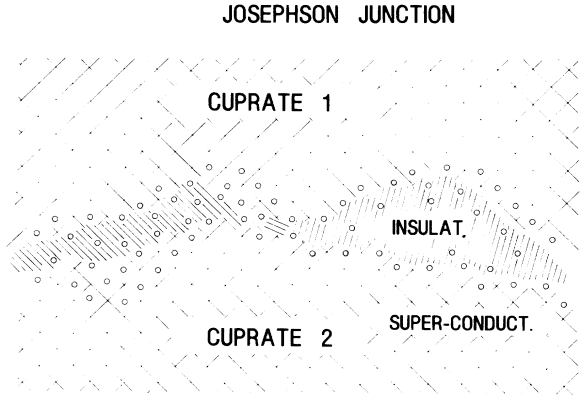


FIG. 1. Sketch of a small part of a planar intergrain (intra) defect along the $CuO_2$ double planes with localized states (0) in the insulator, which mediate a tunnel current. As discussed in Sec. III, at the banks of the cuprate the energy gap of localized states $\Delta_s(x)$ is reduced and thus the supercurrent $j_c$ is reduced, too. The normal current leakage $j_{bl}$ is carried via localized states in the middle of the barrier ($\Delta_s = 0$).

 

copper $d$ levels and oxygen $p$ levels. *Fifth*, O disorder in the Cu-O-chain region, like by more ionic Ba bonds, removes holes from the $CuO_2$ plane, resulting in an insulating phase.[1-3,5] The various types of disorder localize holes in the $CuO_2$ planes. Thus external ("inter") or internal ("intra") interfaces contain a high density of localized states (see Fig. 1).

More specific information about surface and intrinsic interfaces have been inferred in Sec. III from recent tunneling studies on scanning-tunneling microscopy (STM),[9,10] break,[11] and broad area[12-15] junctions. The latter class of "broad area junctions" includes recent studies on intragrain weak links of YBCO.[14,15] The weakly conducting links show up in a grain boundary resistance $R_{bn} \geq 10^{-9}$ $\Omega\,cm^2$, being well above $R_{bn} \approx 10^{-11}$ $\Omega cm^2$ of ideal YBCO grain boundaries. Also the superconducting Josephson current density $j_{cJ} \sim 10^3 - 10^5$ A/cm$^2$ is well below theoretical estimates, i.e., $j_{cJ} R_{bn} \ll \Delta_0/e$, where $\Delta_0 \simeq 20$ meV is the bulk energy gap. In addition $j_{cJ} R_{bn} \propto 1/R_{bn}^m$ $(m \geq 1)$ and $j_{cJ}(T) \propto (1 - T/T_c)^n$ $(1 \leq n \leq 2)$ hold for $a$-$b$ WL. The latter $j_c$ results can be fitted by the proximity effect, i.e., by mean-field considerations, assuming some normal conducting layer.[7] But explanations on a microscopic scale that are able to describe consistently all the results mentioned above, reaching from $\Delta$ degradation and $\Delta$ smearing, tunneling characteristics to interface chemistry, are still missing. First results on the weak charge transfer in $c$ direction[16] with $R_{bn}^{\perp} \sim 10^{-4} - 10^{-5}$ $\Omega\,cm^2$ show properties differing from $a$-$b$ WL with $R_{bn}^{\parallel} \geq 10^{-3}$ $\Omega\,cm^2$.

The atomistic modeling is carried out in Sec. II and III based on the astoninglishly high density of localized states[5] $n_L \leq 10^{21}/cm^3$ in the insulating seam coating cuprate superconductors having a low density of carriers[2] $n_s \geq 10^{21}/cm^3$. The localized states $n_L$ smear out and roughen the metal-insulator interface in approaching the metal-insulator transition (MIT) as in a surface-roughening transition. The interface "roughening transition" is enforced with temperature or voltage. The smearing and roughening of the interface has severe consequences for superconductivity and tunnel channels. As worked out in Sec. II, the Coulomb repulsion by localization weakens superconductivity. This reduces the energy gap and the critical current and causes a normal conducting leakage current to appear—in line with the experiments (Sec. III). For the different tunnel channels Coulomb repulsion and Cooper pair tunneling are outstanding features.

## II. ON TUNNEL EXCHANGE AT CUPRATE SURFACES

In many papers dealing with tunneling between high $T_c$ superconductors,[9-16] barriers are assumed to be rectangular without any internal degrees of freedom. The transmission through such "dead" barriers is described by two parameters: barrier height $\Phi = E_c - E_F > 0$ ($E_c$: conduction band and $E_F$: Fermi energy) and barrier width $d$. The decay constant of wave functions $\kappa_0 = \sqrt{2m\Phi}/\hbar$ yield than the "direct" tunnel current $j_D$ with $n_s$ the density of states[17,18] at the banks:

$$j_D \propto n_s \exp(-2\kappa_0 d)\ . \tag{2.1}$$

"Real barriers," in contrast, are nonuniform $\Phi = \Phi(r)$ and contain internal degrees of freedom, like phonons or localized states $n_L(x,E)$—see Fig. 2. Whereas phonon exchange, i.e., inelastic effects, modulate $j_D$ by percent only,[17] resonant or intermediate-state tunneling $j_I \propto n_L$ surmounts $j_D$ [Eq. (2.1)] drastically.[17,18] While studies on $\Phi(x,y)$ and $n_L(E)$ exist[18,19] for Nb-$Nb_2O_5$ or Nb-$\alpha$Si-$SiO_2$, similar studies do not exist for cuprate superconductors. As a base for such an analysis, we follow Refs. 17 and 18.

To analyze conduction across cuprate surfaces or interfaces the parameters and properties have to be quantified. Concentrating on hole cuprate conductors with $YBa_2Cu_3O_x$ as a model, we follow the $t$-$t'$-$J$ model of Hybertsen *et al.*[20]: The holes reside at O sites of the $CuO_2$ plane, coupling strongly to adjacent Cu and O sites as indicated by the exchange integrals $t > 0.5$ eV in Fig. 3. Based on $p$-$d$ hybridization and the narrow band, these exchange integrals depend strongly on direction, on distance, and on energy of the sites. In addition, they depend on Cu spin because of the Pauli principle.[20] We estimate as Fermi energy $E_F \approx 0.3$ eV and Fermi velocity $v_F \approx 10^7$ cm/sec,[21] despite the fact that correlations and the adjacent MIT make any description of the conducting holes as "Fermi liquid" questionable.[20]

Now, we have to define the nature of the surface of cuprate superconductors. The usually studied surfaces extend parallel to the $CuO_2$ double planes, e.g., at Ba-O stacking faults in YBCO (Ref. 3) or between the Bi-O planes for the Bi cuprates. One reason for these studies is the easy preparation of such inert surfaces by cleaving or deposition. But this inertness corresponds to negligible supercurrent[3] across these "dead", "inert" surfaces.

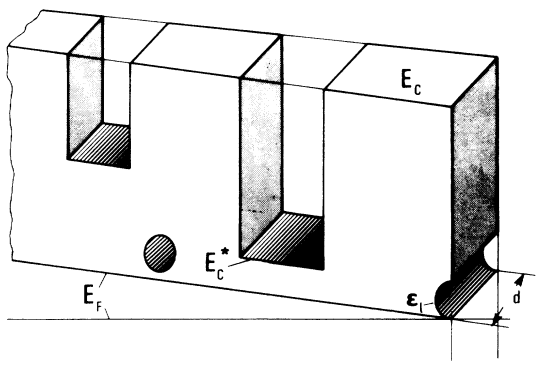


FIG. 2. Sketch of tunnel barriers with $E_c(r)$ the lower edge of the conduction band. Until now barriers $E_c(r) = E_c(x)$ being uniform along the electrodes have been treated, which cannot describe microcrystalline amorphous barriers like $Nb_2O_5$,$\alpha$Si or perturbed YBCO. The model depicted corresponds to $(E_c - E_F) = \Phi \simeq 1$ eV for crystallites, $(E_c^* - E_F) = \Phi^* \simeq 0.1$–$0.2$ eV for channels, and $(E_F - \epsilon_I) \geq 5$ meV for resonant tunneling via localized states symbolized as holes in the barrier. These three entities are the minimum set for the description of a "real" $Nb_2O_5$ barrier.[18] But it is obvious that actual barriers are not steplike and cannot be depicted so simply.

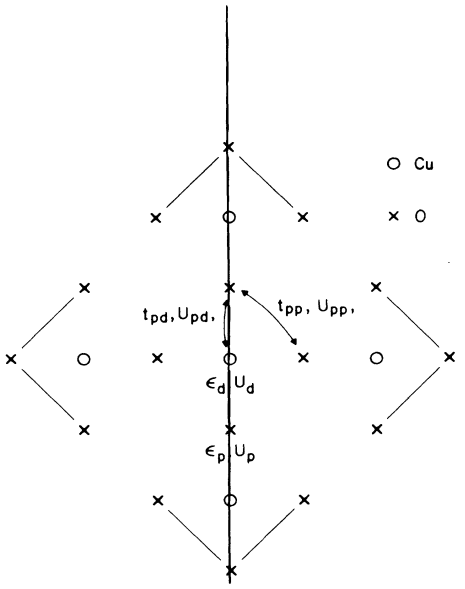


FIG. 3. Largest cluster considered together with the parameters for the three-band Hubbard model[20] in eV: $t_{pd}=1.3$, $t_{pp}=0.65$, $U_d=10.5$, $U_p=4$, and $U_{pd}=1.2$. The Cu-Cu distance is about 0.38 nm and for Cu-O about 0.19 nm.

Such surfaces are no model for conducting cuprate interfaces, i.e., "weak links" shown in Fig. 1. For WL, the makeup of $\hat{a}$-$\hat{b}$ surfaces, especially at the $CuO_2$ planes, is relevant, where not many studies exist. Auger electron spectroscopy, scanning-tunneling electron microscopy, or scanning transmission electron microscopy studies[4] of intragrain weak links showed an intact cation lattice for YBCO. X-ray photoemission spectroscopy (XPS) studies[3] showed a Ba-level shift indicative for hole localization at Ba and no O loss.

### A. Interface states

The electronic conduction across interfaces and the electronic states at *a-b* surfaces are a consequence of the chemistry of the surface or interface. According to Ref. 4 good surfaces keep their cation order and no O loss from a 2 nm thick seam has been observed.[3] That leaves disorder, especially of O in the Cu chains, as an origin for conductivity degradation. This is in line with the observations in single crystals that $T_c$ increases by O ordering even at 300 K,[22] and that O disorder in the "Cu chains" initiates a tetragonal, insulating phase without any O loss.[5] Thus the author proposes as a cause for the insulating layer at external and internal surfaces, relaxation and disorder and the reduced overlap by lattice termination. The localized electronic states in this layer couple now to the adjacent conducting phases forming the interface states (IS). The conducting phase in cuprates is due to mobile holes at the O sites of the $CuO_2$ planes.[20] Their coupling to adjacent "localized holes" in the insulating phase yield IS and tunnel exchange, e.g., with a counterelectrode.

To evaluate the coupling we assume $E_F \sim 0.3$ eV (Ref. 21) and $\Phi = E_c - E_f \sim 2$ eV.[23] This yields as decay width of a localized state in distance $\Delta x$ in front of a homogeneous, conducting phase

$$\Gamma(x) = \frac{0.013 \text{ eV nm}}{\Delta x} \exp(-2\kappa_0 \Delta x) , \tag{2.2}$$

with $\kappa_0 = 7/\text{nm}$ as decay constant. Here *s*-electron-type coupling is much smaller than the exchange integrals $t$ ($>0.6$ V) in Fig. 3 due to the highly directional nature and the correlations in *p-d* hybridization. In the interface the $t$'s of Fig. 3 may hold for the first 0.5 nm due to the finite angular cones and cation order,[1-4] i.e., in the "first 0.5-nm insulator" the decay width $\Gamma(\Delta x)$ depends on local environment with Eq. (2.2) as the lower limit. The dependence on local environment will grow in approaching the MIT, i.e., will roughen the metal-insulator interface, like in the surface-roughening transition. At MIT every property is local. The indirect or resonant tunnel exchange or superconductivity are analyzed in Secs. II B–II D.

### B. Resonant and intermediate-state tunneling

Localized states at energy $E$ and distance $\Delta x$ from the banks in a tunnel barrier couple both banks of the barrier more effectively than the direct tunnel exchange of Eq. (2.1). The largest coherent enhancement is due to resonant tunneling yielding as conductivity for one intermediate state of energy $E_i$ (Refs. 18, 24, 25):

$$G_{\text{res}}(E) = \frac{e^2}{\pi\hbar} \frac{\Gamma^L \Gamma^R}{(E-E_i)^2 + (\Gamma^L/2 + \Gamma^R/2)^2} , \tag{2.3}$$

with $\Gamma^L(\Gamma^R)$ as the decay width to the left (right) bank of the barrier and with $e^2/\pi\hbar$ as the universal conductance scale. The conductivity is largest for $\Gamma^L \simeq \Gamma^R$, i.e., in the middle of the barrier yielding with $n_s$ as density of states in the banks and $n_L(\Delta x, E)$ the density of localized states

$$j_{\text{res}} \propto n_s n_L(d/2, E_F) \exp(-\kappa d) . \tag{2.4}$$

For a uniform distribution of localized states $dn_L(E)/dE = \text{const}$, one obtains:

$$\frac{dG_{\text{res}}}{dV} \approx G_{\text{res}}(V=0) \propto n_s n_L \exp(-\kappa d) . \tag{2.5}$$

Aside from this resonant one-step elastic tunneling, inelastic and multistep processes also occur by, e.g., phonons or excitons or polarons described by the coupling constant $\lambda$. The barrier excitations are needed to bridge localized states at different energies. This inelastic tunneling becomes more likely for larger temperatures $T$, voltages $V$, barrier widths $d$, or density of localized states $n_L$. The self-averaged hopping conductance due to channels involving $n$ localized states is analyzed in Ref. 24 and confirmed experimentally. Important in our context are dependencies on barrier width $d$ and voltage $V$ or temperature $T$:

$$\begin{aligned} &\langle G_n \rangle \propto d^n \exp[-\kappa_0 d 2/(n+1)] , \quad n \geq 1 , \\ &\langle G_n \rangle \propto V^{n-2/(n+1)} \propto T^{n-2/(n+1)} , \quad n \geq 1 , \end{aligned} \tag{2.6}$$

and on coupling constant $\lambda$ and density $n_L$

$$\langle G_n \rangle \propto \lambda^{(n-1)/2} , \quad \langle G_n \rangle \propto n_L^n , \quad n \geq 1 . \tag{2.7}$$

Two-step processes are already large at 4.2 K for extended electrodes as shown by $G_2/G_1 \approx 10$ in $\alpha$-Si.[24] In all the above intermediate-state tunnel processes, small Coulomb charging energies[18]

$$\Delta U^* \ll kT, eU \tag{2.8}$$

are assumed, being estimated at the lower side by the off-site Coulomb energy:

$$\Delta U^* = \frac{0.28d \ [\text{nm eV}]}{\epsilon_r \Delta x (d - \Delta x)} . \tag{2.9}$$

According to the orthodox theory of Berthe and Halbritter and of Likharev,[25,26] $\Delta U^*$ has to be added to the intrinsic energy $E_i$. The relative dielectric constant $\epsilon_r$ in Eq. (2.9) of insulating bulk YBCO of 25 [Ref. 5(b)] is enhanced at interfaces by adjacent interface states with $\epsilon_r \to \infty$ in approaching MIT. There are consequences of the Coulomb charging, which influences tunneling and interface states for $\Gamma(x) < \Delta U^*$ only.[18] So, Coulomb charging in resonant tunneling for $|eU| > \Delta U^*$ reduces the tunnel current by several orders of magnitude.[27] For $|eU| < \Delta U^*$ tunneling is blocked by the so-called Coulomb barrier[18] or blockade.[26] In addition, for $\Gamma(x) < \Delta U^*$, resonant one-step tunneling may have a large inelastic part.[25] The enhancement of $|I(|eU| \geq \Delta U^*)|$ by intermediate states shows slower distance dependencies but stronger voltage dependencies [Eq. (2.6)] than direct tunneling. The channels are easily identified by their different distance dependencies (see STM analysis in Ref. 25 and Sec. III).

### C. Superconductivity and interface states

To model superconductor-insulator interfaces we assume as a boundary the line along Cu-O-Cu as indicated in Fig. 3: on the left, superconductivity; on the right, insulator housing localized states. The localized states (right) at $E_F$ hybridize with conducting states (left) and thus hybridization can be described by the exchange rate $1/\tau = 2\Gamma/\hbar$. We assume that with this rate the "superconductor" and "insulator" properties are averaged. To quantify this we need the superconducting interaction strength, which is not known for cuprates yet.[20,21] We assume an effective interaction constant description with $\lambda_s \sim 2-8$ for the hole superconductivity in YBCO. The insulator property counteracting superconductivity is the Coulomb repulsion. This mechanism is named by Kaiser[28] pair weakening being described by

$$c = \frac{n_L(\Delta x) \cdot U(\Delta x)}{2\pi \Gamma(\Delta x) \int dV n_s \lambda_s} . \tag{2.10}$$

Here

$$\int n_s dV \simeq \tfrac{1}{2} \xi_0^2 n_s \Gamma(\Delta x) 4/11$$

is the number of "superconducting states" in the $CuO_2$ double planes of height 0.4 nm of the 1.1-nm unit cell, in a 90° cone of radius $\xi_0$ = coherence length $\simeq 2$ nm. In Eq. (2.10) $U$ is the on-site (or adjacent-site) Coulomb repulsion, weakening the superconductivity of Cooper pairs localized on one-site—or on adjacent-sites,[21] e.g., O or Cu-O sites in Fig. 3. The gap reduction by pair weakening at localized sites is then described by[28,29]

$$\frac{\Delta_s(\Delta x)}{\Delta_0} = \exp\left[ -\frac{c}{\lambda_s(1-c)} \right] \propto \exp[ -\exp(-2\kappa_0 \Delta x)/\lambda_s ] . \tag{2.11}$$

The gap reduction at localized sites weakens the adjacent superconductivity also. Neglecting local effects for the moment, the mean gap—or $T_c$—reduction of a thin film of thickness $t_s$ by the interface layer is given[29] by a mean $c$ value [Eq. (2.10)]:

$$c(\kappa_0, t_s) = \frac{\overline{n_L} \cdot U_{\text{eff}}}{n_s \cdot t_s \cdot 2\pi \kappa_0 \Gamma_M} , \tag{2.12}$$

with $n_L$ as mean density of localized states in proximity and $\Gamma_M \approx 3 \max[\Delta, kT_c]$ as cutoff for $\Gamma(\Delta x)$.

Aside from pair weakening at localized sites, there exist proposals for negative $U$ centers favoring Cooper pairs[30] despite localization. The negative $U$ centers need a very specific ordered environment to overcome the Coulomb repulsion. They may occur in ordered layered compounds as, e.g., PrBCO or Bi cuprates, discussed in Sec. III. They will show up, e.g., by the "tunnel transfer" of Cooper pairs or $T_c$ enhancements.

### D. Tunneling originating at superconducting cuprate surfaces

In the superconducting state the mean gap reduction [Eq. (2.12)] and the locally reduced gap [Eq. (2.11)] have consequences for tunneling across the interface. Using Sec. II B, the *one-particle tunnel channel* to a counterelectrode yields.

$$j_1 \propto \sum_i n_s(\Delta x_i) f(\Delta_i) \exp[ -2\kappa_0 (d - \Delta x_i) ] \times [ 1 + c n_L (d/2) \exp(+\kappa_0 d) ] , \tag{2.13}$$

with $f$ the Fermi function, $n_s$ the density of bank states, and $n_L$ of localized states. $j_1$ ($U$) carries via $n_s$ information about the local gap values from the cuprate interface. Because of the $\exp[ -2\kappa_0 (d - \Delta x_i) ]$ dependence the most reduced gaps ($\Delta x_i > 0$) in the insulator give a larger (resonant) current than tunneling from the banks ($\Delta x_i < 0$). Because of the high density of localized states $n_L \leq 10^{21}/\text{cm}^2$ and $n_L(E_F) \simeq$ const, resonant tunneling does not falsify the energy-gap information, aside from a possible Coulomb barrier $\Delta U^* < 10$ meV [Eq. (2.9)]. For larger distances, voltages, and temperature, many step processes grow in importance, smearing out the interface information by inelastic processes.[27]

*Cooper pair tunneling* follows a similar sum as Eq. (2.13):

$$j_c \propto \sum_1 n_s(\Delta x_i)\exp[-2\kappa_0(d-\Delta x_i)] \times[1+c_u n_u (d/2)\exp(+\kappa_0 d)] \ . \quad (2.14)$$

Close to the interface $\Delta x_i < 0.2$ nm, Cooper pair tunneling is not changed by the on-site Coulomb repulsion[30] because of $\Gamma > U > 1$ eV. For distances larger than 0.4 nm, $U > \Gamma$ holds for YBCO *a-b* surfaces. Then pair weakening "breaks the Cooper pairs" in a *T*-independent fashion ($kT \ll U$), and thus "Cooper pair resonant tunneling" is suppressed drastically.[30] Only by negative $U$ centers Cooper pairs may be transferred by resonant tunneling described by $c_u n_u$ in Eq. (2.14).

As is obvious from Eq. (2.14), $n_s(\Delta x_i, \Delta_i)$ yields the supercurrent $\Delta_i > 0$. Sites with $\Delta_i \approx 0$ are the origin for a "leakage," i.e., normal current $j_{bl}$. This indirect tunneling via states in the middle of the barrier $j_{bl} \propto n_L(d/2)\exp(-\kappa_0 d)$ together with $j_c$ of (2.14) equals the normal tunnel current. Thus

$$j_c R_{bn} \propto \frac{n_s \exp(-2\kappa_0 d)}{n_s \exp(-2\kappa_0 d) + c n_s \bar{n}_L \exp(-\kappa_0 d)} \propto \frac{\exp(-\kappa d_0)}{\bar{n}_L} \propto \frac{1}{n_s \bar{n}_L^2 R_{bn}} \quad (2.15)$$

holds for $\kappa_0 d \gg 1$. Here $n_L(d/2)$ is a mean density of localized states in the middle of the barrier and $R_{bn}$ the grain boundary resistance. In Eq. (2.15) no negative $U$ centers have been assumed, seemingly valid for *a-b* cuprate surfaces. For coupling of the $CuO_2$ double planes in *c* direction or in YBCO-PBCO-YBCO junctions Cooper pair tunneling via negative $U$ centers seems to be important, as discussed below.

*Electron-hole creation* or scattering at localized sites by intermediate-state tunneling exists[31] in analogy to Andreev reflection.[17] This channel may yield the excess current found experimentally.[32]

## III. COMPARISON WITH EXPERIMENTS

To specify the results of Sec. II the few experimental and theoretical results on cuprate surfaces are summarized. Before doing so, some general comparison between cuprous oxide surfaces and oxidized metal surfaces are in order. *First*, as oxides cuprate surfaces do not oxidize. Instead, they "relax the interface," yielding well-bonded O, as found by XPS.[3] The instantaneous intrinsic relaxation has to be contrasted to natural oxidation of metals being extrinsic, taking time (> 100 min) and shifting defects out of the oxide.[18] *Second*, because of the two-dimensional structure and because of the highly direction *p-d* hybridization YBCO has a narrow, two-dimensional conduction band and small carrier density $n_s > 10^{21}/\text{cm}^3$ close to MIT. *Third*, relaxed surfaces will render the cuprate insulating due to the reduced hybridization by a surface or by disorder, or perturbations related, e.g., to O relaxation or strain. This interface layer contains localized states at $E_F$, and as an estimate for their density $n_L$, distances between localized sites of 0.5–1 nm reduce $n_s$ to $n_L \leq 10^{21}/\text{cm}^3$. The small difference between $n_s \geq 10^{21}/\text{cm}^3$ and $n_L \leq 10^{21}/\text{cm}^3$ has to be contrasted to $n_s > 10^{22}/\text{cm}^3$ and $n_L < 10^{18}-10^{16}/\text{cm}^3$ found for classical three-dimensional metals and their oxide coatings.[17,18] The large ratio $n_s/n_L > 10^4$ yields a sharp metal-oxide interface, which allows easy identification of tunnel channels originating either in the metallic banks or in the insulator.[18] In contrast, for YBCO $n_s/n_L \geq 1$ yields a smeared out and roughened metal-insulator interface with an adjacent high density $n_L$. Thus the different tunnel channels are not separable by the standard methods discussed in Refs. 17 and 18.

Below it is shown that all tunnel results on external or internal surfaces of YBCO known to the author comply with the above-developed formulas. Independent evidence on localized states by disorder is coming from *specific-heat* measurements, which by radiation damage, show no normal conducting phase but ample evidence for localized states;[33] or XPS shows at YBCO interfaces[3] localization of holes at Ba yielding localized states in the $CuO_2$ planes. In contrast to YBCO, Bi cuprates are more inert, i.e., don't show relaxation induced by the reactive Ba. This may be the reason for "stronger weak links" with less leakage current.[9] The difference in inertness at the Ba or Bi planes corresponds not only to a smaller leakage current but also to easier cleavage of Bi cuprates and higher mechanical and chemical stability of Bi cuprates. The above comparison deals with the intrinsic relaxation only. Extrinsic reactions with various agents are known but are beyond the scope of this paper.

Before analyzing the transport via localized intermediate states depicted in Fig. 4, their "local energy gap" is estimated according to Sec. II C. With Coulomb repulsion on site $U_{pp} \simeq 4$ eV and adjacent site $U_{pd} \simeq 1.2$ eV, $\lambda_s \approx 2-8$, $t \approx 0.65$ eV/2 (Fig. 3), and $n_s \geq 10^{21}/\text{cm}^3$, Eq. (2.10) yields for states localized in $\Delta x \approx 0.2$nm distance:

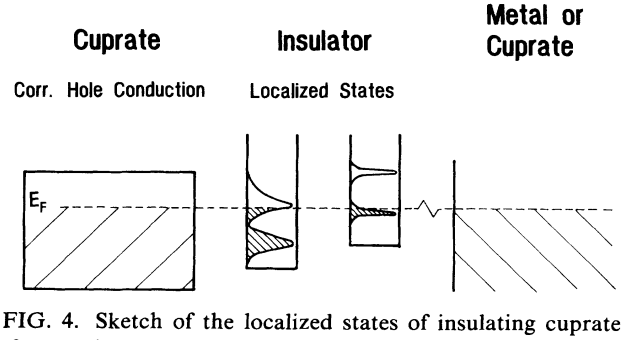


FIG. 4. Sketch of the localized states of insulating cuprate surfaces at internal or external surfaces. By angle, distance, or energy disorder and by the very existence of a surface, states become localized and show weakened hybridization with the cuprate. These states transfer current by resonant or intermediate tunneling hindered by a Coulomb barrier at low voltages. Correlated electron-hole tunneling via localized states does not show this barrier and thus is large growing with the amount of localized states, i.e., with the insulator thickness as compared to the resonant tunneling with its Coulomb barrier $\leq 10$ meV. By Coulomb repulsion the superconductivity of the bulk ($\Delta_0$) is weakened in the first ordered layer of localized states ($\Delta x \approx 0.19$ nm) to $\Delta_s \approx \Delta_0/4$ allowing Cooper pair resonant tunneling. The next layer ($\Delta x \approx 0.38$ nm) shows $\Delta \approx 0$ and thus transfers mainly the normal leakage current $j_{bl}$.

$$c_{pp} \simeq 0.6-0.16 \quad \text{or} \quad c_{pd} \simeq 0.18-0.05 \ . \tag{3.1}$$

Then Eq. (2.11) (Refs. 28, 29) yields for the first layer of localized states as surface energy gap $\Delta_s$ (Fig. 4)

$$\Delta_s/\Delta_0 \simeq 0.4-0.9 \quad \text{or} \quad \Delta_s/\Delta_0 \simeq 0.9-0.95 \ . \tag{3.2}$$

For the next layer ($\sim 0.4$ nm) of localized states the averaged decay width $\Gamma$ of Eq. (2.2) seems more appropriate than estimates by directional hybridization (Fig. 3). With $\Gamma(0.4\ \text{nm}) \approx 10^{-3}$ eV or the $t$ values of Fig. 3, Eq. (2.10) yields $c > 5$, i.e., $\Delta_s \approx 0$, by the double exponential decay in Eq. (2.11). In short, states in distances larger than $\Delta x \simeq 0.4$ nm from the superconducting cuprate are "normal conducting." For states closer ($< 0.3$ nm) to the $\hat{a}\hat{b}$ surface by the order, a well-defined surface energy gap $\Delta_s/\Delta_0 \approx 0.4$ exists. Such surface states depress in a local fashion the energy gaps "$\Delta_0$" of the cuprate banks.

For a thin YBCO layer the pair weakened interface seam effectively depresses $\Delta$ and $T_c$ according to Eq. (2.12). For example, one estimates $T_c^* \approx 20$ K for well-ordered O plackets of only 1-nm size. This may explain the $T_c$ growth with $x$ and the $T_c$ growth by annealing of $YBCO_{7-x}$.[22] In regions farther than 0.4 nm away from the metallic cuprate, an off-site Coulomb barrier (2.9)

$$\Delta U^* \simeq \frac{0.28d\ [\text{nm eV}]}{\epsilon_r \Delta x (d-\Delta x)} < 10\ \text{meV} \tag{3.3}$$

occurs, where $\epsilon_r \approx 100$ is assumed because of the close-by IS and MIT.

### A. One-particle tunneling: barrier properties

In classical tunnel junctions the analysis of the $I(U)$ characteristics is an accepted, successful method to identify either barrier properties or properties of the metallic banks.[17,18,24] The barrier properties obtained are barrier shape, localized states density $n_L(\Delta x, E)$,[18] and electron-phonon coupling.[17,24] Metal properties obtained are density of states $n_s(E)$ and electron-phonon coupling.[17] The easy separation for classical junctions is based on distinct voltage dependencies of different tunnel channels due to $n_s/n_L > 10^4$. In contrast, at cuprate surfaces $n_s/n_L \approx 1$ holds, which is the reason for so many unsuccessful attempts to analyze tunnel data. To identify different unknown tunnel channels out of the $U$ dependence of Eqs. (2.1)–(2.7) (Refs. 17, 18, 24) seems impossible because, e.g., $\kappa(E)$ depends on voltage also. But by additionally changing the barrier width, the situation becomes clear. This actually can be seen in Fig. 5, showing $I(U,d)$ of Bi cuprates.[9] For the smallest distance, direct tunneling with $dI/dU \approx 0$ for $|U| > 0.25$ V fits to a conduction bandwidth of about 0.25 eV.[21] With increasing tip-cuprate distance, $dI/dU$ changes from a decrease above $\pm 0.1$ V caused by a $n_s(|E-E_F|)$ decrease to a slight increase proportional to $|U|^\alpha$ ($\alpha > 0.3$). Here $\alpha$ increases with distance whereas the onset of $|U|^\alpha$ decreases with distance $d$. This is in accordance with Sec. II B with a large density of localized states $n_L$ and a "inelastic coupling" via phonons or polarons. The density of states seems to be "white $n_L(E) \simeq$ const" up to 0.5 eV, causing $dI/dU \propto U$ ($\leq 0.5$ V) as background conductance.[9–13]

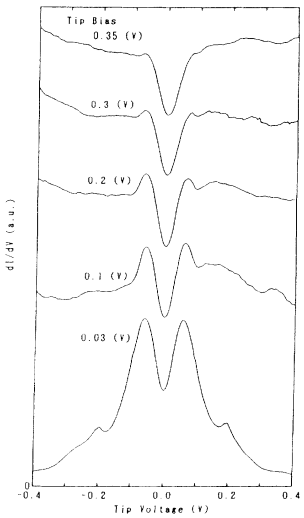


FIG. 5. Bias voltage dependence of the STM tunnel spectrum of the cleaved surface of Bi-Sr-Ca-Cu-O at 4.2 K. Larger bias voltages correspond to larger distances. The obvious increase of $G = dI/dU$ above 0.2 V with distance, i.e., with bias, is explained by an increasing number of intermediate states involved in tunneling. Such states are not active for the smallest distances (0.03 V) and thus the constant current $I(U) > 0.2$ V may reflect a Fermi energy of 0.2 eV.

The STM result on Bi cuprates[9] with a minimal leakage current $j_{bl}$ of 5% as compared to the normal current have to be contrasted to YBCO showing much larger leakage currents ($\sim 10\%-90\%$) and no clear downset $dI/dU \approx 0$ above 0.3 V.[10] We explain this difference by a smaller density of localized states $n_L$ of the "more inert Bi cuprates." The higher density $n_L$ for YBCO yields also a much more uniform $dI/dU \propto U$ dependence, especially observed in $\hat{c}$ direction up to $0.5V$.[10] The $dI/dU \propto U$ dependence overshadows any Coulomb barrier below 0.01 V (Refs. 12, 13) or excess currents.[32] That is, current offsets like in STM (Ref. 25) or broad area $\alpha$-Si barriers[27] are difficult to detect and excess currents may not implement metallic contact.[32]

Besides the voltage dependencies of the tunnel current discussed above, the distance dependencies also prove the existence of many intermediate states in series. Whereas the $U$ dependence of $I$ in STM indicates a barrier $\Phi \simeq 2$ eV (Ref. 23), the actual decrease $I(\approx 0.5\ \text{V}, d)$ with distance yields $\Phi^* \simeq 0.3$ eV, assuming direct tunneling [Eq. (2.3)]. The ratio $\Phi/\Phi^* \approx 7$ links to hopping via 1 to 2 intermediate states being likely for the STM conditions[23] 300 K and 0.5 V.

In addition to the above STM-$I(U,d)$ results, break area or broad area junctions and intergrain or intragrain weak links also conform to a high density of localized states $n_L \leq 10^{21}/\text{cm}^3$. To outline this, the grain boundary resistance $R_{bn}$, the Josephson critical current $j_c$, and the normal-state leakage tunneling $j_{bl}$ have to be introduced. For intragrain weak links[14,15] $R_{bn} \geq 10^{-9}\ \Omega\,\text{cm}^2$ are found. Comparing this with $10^{-12}\ \Omega\,\text{cm}^2$ found for Nb-Nb grain boundaries,[34a] $n_s \approx 4.\ 10^{21}/\text{cm}^3$ for clean metal-

lic YBCO-YBCO grain boundaries yields $R_{bn}^{*} \approx 10^{-11}$ $\Omega\,\mathrm{cm}^2$ as the Sherwin resistance. The enhancement from $10^{-11}$ to $10^{-9}$ $\Omega\,\mathrm{cm}^2$ can be explained by resonant tunneling across 1-nm insulator with $\Phi \simeq 2$ eV and $n_L \approx 10^{21}/\mathrm{cm}^3$. The YBCO intragrain weak link resistance increases with oxygen loss[15] to $R_{bn} \approx 10^{-7}$ $\Omega\,\mathrm{cm}^2$. This drastic resistance increase by a factor up to 100 is accompanied by an increase of $d\rho/dT$ by a factor of 2 only.[22] The $R_{bn}$ increase by a factor of 100 is explained by an increase of the barrier width $d$ entering exponentially. The increase of $d$ is due to a density of state decrease $n_s \propto 1/d\rho/dT$ because the metal-insulator interface retracts with a reduced overlap and close-by MIT. It should be mentioned that the O content of the interface does not change,[3] i.e., $n_L$ does not decrease, only $n_s$ decreases. $SrTiO_3$ bicrystal YBCO weak links[14] show $R_{bn} \geq 10^{-8}$ $\Omega\,\mathrm{cm}^2$ increasing with angle $\theta$, which hint to wider barriers than for the more intrinsic weak links.[15] Intergrain weak links show[12] $R_{bn} > 10^{-7}$ $\Omega\,\mathrm{cm}^2$, which can be explained by a barrier width $d \simeq 2$ nm and $n_L \geq 10^{20}/\mathrm{cm}^3$—as compared to $d \simeq 1$ nm for intragrain WL's.[34(b)] Intrinsic perpendicular tunneling is weak because the $p$-$d$ hybridization is confined to the $CuC_2$ double planes. This is confirmed by single crystals of Bi cuprates[16] showing $R_{bn}^{\perp} \simeq 10^{-4}$ $\Omega\,\mathrm{cm}^2$ being several orders of magnitude larger than $R_{bn}^{\parallel}$ for $\hat{a}$-$\hat{b}$-WL.

### B. One-particle tunneling and superconducting energy gap

In approaching the MIT, the directional $p$-$d$ bonding in the $CuO_2$ planes with $n_s \geq 10^{21}/\mathrm{cm}^3$ in proximity to a high density of localized states $n_L \leq 10^{21}/\mathrm{cm}^3$ yields a surface roughening transition of the metal-insulator interface. The roughness increases with $T$, $U$, and reduced $n_s$. Thus with increasing temperature and voltage, decreasing $n_s$, and with approaching $T_c$ from below, the effective tunnel barrier width $d$ widens. This has been found experimentally.[13,20,32] The "roughening transition" of the metal-insulator interface is accompanied by locally varying energy gaps [Eq. (3.2)] with $\Delta^{*}(x)$ decaying fast ($\sim 0.5$ nm) into the insulator. The ensemble of varying energy gaps $\Delta^{*}$ has a characteristic smearing width $\delta\Delta$ which is described in Ref. 35 by $\Delta_0$-$i\Gamma_\Delta$. As described in Eq. (2.13), the gap distribution or smearing $\Delta_0$-$i\Gamma_\Delta$ measured by tunneling is weighted by $\exp[-2\kappa_0(d-\Delta x)]$ enhancing the weight of IS with small $\Delta_0 - \delta\Delta(\Delta x)$. Fits to $I(U)$ of break junctions[11–13] and STM[9,10] yield $\delta\Delta \approx 5$ meV $\approx \Delta_0/4$. This value is the saturation value observed for classical superconductors approaching the metal-insulator transition (MIT).[35] Our explanation of smearing by a "gap roughening" in approaching MIT explains[35] $\Gamma_\Delta \propto 1/\sigma$ in a natural way by a reduced overlap $\propto 1/\sigma$ occurring at the interface. The agreement[13] $\delta\Delta \approx \Delta_0/4$ with the characteristic surface energy gap $\Delta_s$ [Eq. (3.2)] should be mentioned. In addition, junctions of larger width show more smeared-out gap structures by intermediate-state tunneling.

### C. Critical Josephson current $j_c$ and leakage current $j_{bl}$

The supercurrent across a junction is given by Eq. (2.14), where the "gap roughening" is exponentially weighted $\propto \exp[-2\kappa_0(d-\Delta x)]$. The different Cooper pair channels in parallel yield [Eq. (2.14)]

$$j_c \simeq \frac{C^{*}}{R_{bn}} \sum_i \Delta_i \exp[-2\kappa_0(d-\Delta x_i)] = \frac{\overline{\pi\Delta^{*}}}{cR_{bn}2e} \tanh \frac{\overline{\Delta^{*}(T)}}{2kT} , \tag{3.4}$$

with $\Delta^{*}$ as fit constant for $c=1$. The fit constant $\Delta^{*}$ is not related to an energy gap $\Delta_s$ of Eq. (3.2) directly or in any averaging sense. This is not only because of the exponential weighting (3.4), but also because $R_{bn}$ [Eq. (2.13)] is dominated by resonant tunneling [$\propto \exp(+\kappa_0 d)$]. Experimentally $\Delta^{*}$ has a maximum of 8 meV for YBCO,[14,15] and is different from the surface energy gap $\Delta_s$. Experimentally, from the temperature dependence $j_c(T) \propto \exp(-\Delta_s/kT)$ of bicrystal weak links[14] or from penetration depth analysis[36] $2\Delta^{*}/kT_c \approx 2$, i.e., $\Delta_s = \Delta^{*} \approx 5$ meV, is obtained for $T \leq T_c/4$. $\Delta_s$ is in agreement with surface energy gap from tunneling[13] and with the smearing $\delta\Delta$ discussed in Sec. III B. Temperature dependencies above $T_c/4$

$$j_c(T) \propto (1-T/T_c)^m , \quad (1 \leq m \leq 2) , \tag{3.5}$$

have been found, where smaller $m$ are found for better junctions.[14,15] Often $m \simeq 2$ holds ($T \geq T_c/2$), which/p is explained by superconductor-normalconductor-superconductor junctions.[7,8] Close to $T_c$ the roughening of the cuprate-insulator interface and $\Gamma_\Delta \simeq \Delta_0/4$ (see above) smear the interface over about 1 nm and thus a mean-field treatment (proximity effect) is equivalent to our metal-insulator and pair weakening description.

States farther away from the cuprate ($\geq 0.5$ nm) are "normal conducting," i.e., they weaken the Cooper pair tunnel current to zero [see Eq. (2.11) and Fig. 4]. These states carry the so-called leakage or normal conducting current. We assume

$$j_{bl} \simeq j_{bn} - j_c = j_{bn}\left[1 - \frac{1}{c}\right] , \tag{3.6}$$

with $j_{bn}$ ($\propto 1/R_{bn}$) the tunnel current in the normal state and $c$ is given in Eq. (3.4) by using $\Delta^{*} = \Delta_0$. For typical intergrain weak links $c > 100$ holds[34] and only for intragrain weak links $c \approx 1$ is obtained.[14,15] Minimal numbers for $j_{bl}/j_c$ are 5% for Bi and 10% for Y cuprates[9,10] obtained by STM, whereas broad area junctions shows values above 50%.[13,34] Hence in most cases, the "normal conduction" leakage current dominates, which is due to the fact that

$$j_{bl} \propto n_s n_L \exp(-\kappa_0 d) \propto j_n \propto 1/R_{bn}$$

decays with $d$ more slowly than $j_c \propto n_s \exp(-2\kappa_0 d)$ and that $n_L \approx n_s$ holds. The dependence $j_c R_{bn} \propto 1/R_{bn}$ [Eq. (2.15)] has actually been observed by deoxygenation enhancing $R_{bn}$ from $10^{-9}$ to $10^{-7}$ $\Omega$cm$^2$.[15] Thus deoxygenation of YBCO enhances $d$ by reducing the O content and $n_s$ in the bulk, whereas $n_L$ and the surface O content do not change.[3] Bicrystals show $R_{bn} \geq 10^{-8}$ $\Omega$ cm$^2$ and $j_c R_{bn}(\theta) \propto 1/R_{bn}^{1/2}(\theta)$ with $\theta$ the grain boundary angle. According to Eq. (2.15) $R_{bn} > 10^{-8}$ $\Omega$ cm$^2$ hints to a wider insulator gap and the exponent 1.2 to a dependence of $n_L$ on $\theta$. With oxygenation $j_c R_{bn}$ can be enhanced for the bicrystal weak links also.[37] For Nb-$Nb_2O_5$ junctions $j_c R_{bn} \propto 1/R_{bn}$ by resonant tunneling has been found also.[18]

All the above tunnel studies assume uniform barriers, which do not occur in nature. These nonuniformities are not only the averages over the roughened transition layer on a scale below 1 nm [Eqs. (2.13) and (2.14)], but also strong $d$ and $n_L$ variations occur along real junctions on a scale above 2 nm, obvious from high resolution transmission electron microscopy results.[14] Thus Eq. (3.4) may be substituted by

$$\overline{j_c} \propto \overline{\sum j_c^i} \overline{\sum 1/c_i R_{bn}^i} = c^* \sum_i n_s^i \exp(-2\kappa_0 d_i) \sum_i^n \frac{\exp(+\kappa_0 d_i)}{n_s^i n_L} . \quad (3.7)$$

Because of the exponential dependencies the shortest $d_i$ with the largest $n_s$ and smallest $n_L$ always dominates. These dominating tunnel spots of sizes around 1–2 nm are proposed by the author[41] as origin for the so-called "microshorts" or better "nanoshorts" with $j_{cj} > 5 \times 10^7 A/\text{cm}^2$ able to carry current above 10 T.

Resonant tunneling via states in distances larger than 0.5 nm are accompanied by charging of the localized site, which then senses the charging of adjacent two level systems of the insulator.[38] Thus, noise will be proportional to the leakage current $j_{bl}$ sensing the two level systems via localized states more directly. This dependence[18] on $j_{bl}$ has been observed in Nb junctions[38] and in YBCO junctions.[37] The large density $n_L$ and large $j_{bl}$ for YBCO did not allow the identification of individual telegraph noise flicker states found for Nb-$Nb_2O_5$.[38]

The noise ($\propto j_{bl}$) (Refs. 37–39) corresponds to $rf$ residual losses $R_{\text{res}}$, in line with the fluctuation-dissipation theorem. For bulk superconductors $R_{\text{res}}$ has been cast in the equations[34]

$$R_{\text{res}} \propto \omega^2 \lambda_J^3 j_{bl} \propto R_{bn}^2 \quad \text{and} \quad \lambda_J \propto 1/\sqrt{j_c} \propto R_{bn} \quad (3.8)$$

with $\lambda_J$ the Josephson penetration of the weak links. This dependence has been found for cuprate superconductors with their large values of $j_{bl}/j_c \simeq 50\%$ and in Nb and NbN cavities with $j_{bl}/j_c \simeq 1\%$.[34a] To reduce noise and $R_{\text{res}}$ small $j_{bl}$, i.e., small grain boundary resistances $R_{bn} < 10^{-9}$ $\Omega$ cm$^2$, are advantageous—see, e.g., Eq. (3.8). Thus a small number of nanoshorts with $R_{bn} \leq 10^{-9}$ $\Omega$ cm$^2$ is superior to many junctions or extended junctions with $R_{bn} > 10^{-9}$ $\Omega$ cm$^2$ in parallel.

Junctions with low noise and small $R_{bn}$ have been found in epitaxial films[14] or in step edge junctions.[39] As is obvious from the outlined "intermediate-state tunnel channels," the above model is not only applicable to $\hat{a}$-$\hat{b}$ weak links depicted in Fig. 1. The model applies to all junctions with appropriate intermediate states, as, e.g., the 90° step edge junctions,[39] $\hat{a}$-axis films,[40] or trilayers junction with tunneling perpendicular to the $CuO_2$ double planes.[16(b)]

### D. Comparison with other junction models

Two other models are used to describe cuprate weak links and junctions: proximity-effect models assuming a normal conducting layer or a normal layer with spin-flip scattering.[7,8] Both models deal mainly with the $T$ dependence of $j_c(T)$ and with the depression of $j_c = j_{bn}/c$ relative to $j_{bn}$ [Eqs. (3.4) and (3.5)]. They do not deal with the large leakage current directly, which is experimentally weakly depending on $T$ and $H$ field.[34]

First, above $T_c/2$ our microscopic model is equivalent to proximity-effect–mean-field models in using the appropriate energy transfer between superconductor and localized sites [Eqs. (2.10)–(2.12)]. Second, the strong Coulomb repulsion $U > 1$ eV yields a temperature-independent degradation $c \gg 1$ in less than 1-nm thickness. In contrast, normal conduction ($\lambda_s = 0$) needs a sheath of more than $10\xi_n$ thickness to yield, e.g., $c > 10$. A spin-flip layer ($\lambda_s < 0$) needs about $3\xi_n$ as thickness with $\xi_n$ the coherence length in those layers.[8] Taking as minimum number for $\xi_n \simeq 1$ nm, i.e., the length where transition metal oxide may obtain stoichiometry, we obtain 10 nm or 3 nm as "normal layer" coating on the cuprate. Such a layer has not been observed[3,4] as summarized in the Introduction. The facts that both models[7,8] would yield $j_{bl}(H)$ dependencies not found[34] and because both models cannot explain the noise $\propto 1/R_{bn}$,[14,37] the rf residual losses (Ref. 34) $\propto R_{bn}^2$ and $j_c \leq 10^6$ A/cm$^2$ for 90° junctions,[39] our pair weakening by Coulomb repulsion at $\hat{a}$-$\hat{b}$ plane interfaces seems a better description for cuprate weak links.

### E. Normal and supercurrent perpendicular to the $CuO_2$ planes

So far, most Josephson junctions and WL use the high $p$-$d$ conductivity along the $CuO_2$ planes.[14,15,37,39–41] Such grain boundary junctions, if clean, should show $R_{bn} \approx 10^{-11}$ $\Omega$ cm$^2 \propto n_s$. But the intrinsic instability of $\hat{a}$-$\hat{b}$ surfaces discussed above yield $R_{bn} > 10^{-9}$ $\Omega$ cm$^2$, $j_c$ depression by $10^1$–$10^4$ and a leakage current $j_{bl} \geq j_c$. The situation is different perpendicular to the $CuO_2$ planes. There, the easy cleavage proves the existence of inert surfaces with negligible dangling bonds, i.e., order is maintained. Thus, a negligible amount of localized states causing pair weakening may exist. This is confirmed by high quality $Bi_2Sr_2CaCu_2O_8$ (2212) single crystals showing[16(a)] for $j_c^\perp$ Josephson coupling $\Delta_0 \approx 20$ meV and $R_{bn}^\perp \approx 10^{-4}$ $\Omega$ cm$^2$, i.e., a large energy gap and resistance. Not optional growth conditions reduce some $\Delta$ values and enhance $R_{bn}^\perp$ hinting to defects causing pair weaken-

ing and tunneling.

In a well-defined way by ALL-MBE[16(b)] $j_c^{\perp}$ junctions have been grown where defects have been introduced by a doped ($22n\ n+1$) barrier between (2212) electrodes. For $d \sim 3$ to 5 nm $R_{bn}^{\perp} \sim 10^{-5}$ to $10^{-2}\ \Omega\,\mathrm{cm}^2$ have been obtained, which is in accordance with resonant tunneling [$\propto \exp(-\kappa_0 d)$] with $\Phi \simeq 2$ eV. Important is the result[16(b)] of $I_c R_{bn} \simeq 0.5$ mV $\simeq$ const for $3 \le d \le 5$ nm proving that single particles for $T > T_c$ and Cooper pairs for $T < T_c$ use the same tunnel channel. For $d > 6$ nm $I_c$ was not detected but hints to two-hop intermediate-state tunneling are found.[24] Thus, the ordered and doped ($22n\ n+1$) barriers[16b] contain intermediate states of negative $U$ center type with $\Delta^* \approx 1$ meV supporting superconductivity. The very existence of $U$ centers is related to well-ordered and molecularly defined barriers.

YBCO has not yet achieved a quality needed for Josephson effect measurements using $j_c^{\perp}$. This seems related to the higher density of localized states due to the reactivity of Ba[3]. The localized states cause $R_{bn}^{\perp} \approx 10^{-7}\ \Omega\,\mathrm{cm}^2$ (Ref. 41) and metallic conductivity $p^{\perp} > 3\ \mathrm{m}\,\Omega\,\mathrm{cm}$ and a reduced energy gap $\Delta^* < $ meV by pair weakening. The large extrinsic conduction $R_{bn}^{\perp} \approx 10^{-7}\ \Omega\,\mathrm{cm}^2$ shunts the intrinsic $R_{bn}^{\perp} \simeq 3 \times 10^{-6}\ \Omega\,\mathrm{cm}^2$. This $R_{bn}^{\perp}$ estimate is based on a barrier between the $CuO_2$ double planes of width $d \simeq 0.8$ nm and $\Phi \simeq 2$ eV using $R_{bn} \approx 10^{-4}\ \mathrm{cm}^2$ of (2212).[16(a)]

### F. YBCO-PBCO-YBCO junctions

$Y_{1-x}Pr_xBa_2Cu_3O_7$ is known[42] as a superconductor for $x \le 0.6$ with a $T_c$ decreasing roughly linearly with $x$. YBCO, like the other rare-earth derivates $R_{1-x}Pr_xBa_2Cu_3O_{7-x}$, shows a similar decrease with $x$.[42] The initial $T_c$ and the $T_c$ decrease with $x$, which are both independent of the magnetic moment of "$R$", show that pair breaking is neither occurring in RBCO nor the reason for the decrease with $x$ for $Y_{1-x}Pr_xBCO$. The decrease $T_c(x)$ for the latter seems to follow the same road as the decrease of $T_c(x)$ of $YBCO_{7-x}$. Not only are both turning insulating at $x \approx 0.5$ but also the mechanisms of becoming insulating seem identical as shown by the Ba-XPS level shift[3,43] and by the conductivity decrease. The XPS Ba level shift shows that in both cases the density of conducting holes in the $CuO_2$ planes are reduced. Thus the author proposes that the $T_c(x)$ decreases of $Y_{1-x}Pr_xBCO_7$ and of $YBCO_{7-x}$ are both due to pair weakening by localized sites of insulating parts growing with $x > 0.1$. According to Eq. (2.11) (Ref. 29) pair weakening by on-site or adjacent-site Coulomb repulsion yields the linear $T_c$ decrease with $x$, as observed experimentally.[22,42]

Based on these general remarks about superconductivity and its weakening by becoming insulating, the PBCO junctions are discussed. Epitaxial films on PBCO and YBCO can be grown by identical methods at similar substrate temperatures without breaking the vacuum.[44] A high density of localized states[44,45]

$$n_L \le 10^{20}/\mathrm{cm}^3 \tag{3.9}$$

has been inferred from the activated conduction along the $\hat{a}$-$\hat{b}$ direction. This activated conduction becomes $T$ independent below 100 K in PBCO tunnel barriers ($< 1\ \mu$m), which is in line with Eq. (2.6) and Ref. 24, where the temperature dependence by multistep processes became prominent for $|kT| > 10$ meV only. The conduction in PBCO is supported by the YBCO banks as shown by[44] $\rho \simeq 0.4\ \Omega\,\mathrm{cm}$ for $d \le 10$ nm ($R_{bn} \simeq 3.10^{-7}\ \Omega\,\mathrm{cm}^2$) and 4 $\Omega\,\mathrm{cm}$ for $d \ge 20$ nm ($\simeq 10^{-5}\ \Omega\,\mathrm{cm}^2$). Here 4 $\Omega\,\mathrm{cm}$ already corresponds to bulk values.[42a] The "induced conduction" in PBCO has a characteristic length $d_p \simeq 5$ nm, which seems to correspond to the decay of the supercurrent for $d \ge 2d_p$ (Ref. 44).

$$j_c(d) \propto \exp(-d/\xi_p) \quad \text{with } \xi_p \simeq 10 \text{ nm}\ , \tag{3.10}$$

$$j_c R_{bn} \propto 1/R_{bn}^m \quad \text{with } m \approx 0.2\ . \tag{3.11}$$

A barrier of $d > 5$-nm width cannot be crossed by direct tunneling. Hence, the exponent $m \approx 0.2 < 1$ shows that in PBCO single holes above $T_c$ and Cooper pairs below $T_c$ use the same tunnel channels. To solve the puzzle of "induced" conduction in the normal ($d_p \simeq 5$ nm) and superconducting state ($\xi_p \simeq 10$ nm) (Ref. 42) the order of PBCO may be the key point. The order may yield the "conducting PBCO pockets."[42a] The ordered PBCO pockets of sizes $\le 2$ nm show attractive Cooper pair interaction in the sense of a negative $U$ center.[30] In addition, evidence is mounting that superconductivity in $YBCO_{7-\delta}$ also needs pockets of $6 \times 6$ chain oxygen in the ortho-II phase to yield superconductivity.[46]

## IV. CONCLUSION

Classical metals are broadband, three-dimensional conductors ($n_s > 10^{22}/\mathrm{cm}^3$) and show a oxidized surface with a smooth but abrupt spacewise metal-insulator transition. In contrast, the new cuprate superconductors have a narrow, quasi-two dimensional $p$-$d$ conduction band with a low carrier density ($n_s \ge 10^{21}/\mathrm{cm}^3$) close to the metal-insulator transition (MIT) occurring in two dimensions already for $n_L \le 10^{21}/\mathrm{cm}^3$ as density of localized states. Thus any perturbation of the delicate $p$-$d$ hybridization, i.e., of spatial, energetical, and directional order, renders the cuprates insulating. Such perturbations occur at internal or external $\hat{a}$-$\hat{b}$ surfaces by intrinsic relaxation or strain fields or by the very existence of that surface. All this yields an insulating seam ($\ge 1$ nm) with $n_L \le 10^{21}/\mathrm{cm}^3$. The high density of localized states $n_L$ in proximity with a low density of conducting states yields a smeared-out metal-insulator interface and an interface roughening transition with increasing $T$ and $U$ in approaching MIT. Thus the grain boundary resistance is with $R_{bn} > 10^{-9}\ \Omega\,\mathrm{cm}^2$ always enhanced over the intrinsic $R_{bn} \approx 10^{-11}\ \Omega\,\mathrm{cm}^2$, and this $R_{bn}$ will grow with degradation. Localized "Cooper pairs" in the seam show depressed superconductivity by on-site Coulomb repulsion giving rise to locally varying (roughened) energy gaps $\Delta_s < \Delta_0$ and to a depressed Josephson critical current $j_c(T)$. As counterpart to the $j_c(T)$ depression, a large leakage current $j_{bl}/j_c \propto 1/j_{bl} \propto R_{bn}$ occurs by reso-

nant tunneling via states with $\Delta_s = 0$. This large leakage current causes excess noise ($\propto j_{bl}$), excess rf residual losses ($R_{\rm res} \propto j_{bl} R_{bn}^3 \propto R_{bn}^2$), and $j_c$ depression ($j_c \propto j_{bl}^2$). For $T > T_c/4$ the temperature decrease of $j_c(T)$ can be fitted by mean-field theories based on pair weakening.

In contrast to $\hat{a}$-$\hat{b}$ interfaces, the intrinsic conduction perpendicular to the $\hat{a}$-$\hat{b}$ planes is small ($R_{bn} > 10^{-5}$ $\Omega\,\mathrm{cm}^2$), but often not degraded by the lack of localized states. The occurrence of such defects enhances the conduction to $R_{bn} \approx 10^{-7}$ $\Omega\,\mathrm{cm}^2$ with weakened superconductivity occurring especially for YBCO.

Beside localized states causing pair weakening, also negative $U$ centers also exist, supporting superconductivity by resonant tunneling over distances in excess of 3 nm. The first evidence for this phenomenon was found in Nb-$\alpha$Si-Nb junctions[19] already, where Si negative $U$ centers have been proposed by theory.[47] These negative $U$ centers may also serve as explanation for $T_c$ enhancements by adjacent $\alpha$Si (Ref. 48) or for the superconductivity in cuprates. Tunneling gives evidence for negative $U$ centers in ordered doped Bi cuprates and PBCO.

The consequences worked out above of an intrinsic density of localized states at surfaces hold not only for two-dimensional cuprates but also for the three-dimensional bismuthates. In this case the tunnel barrier is prepared by irradiation,[49] i.e., by disorder, producing plenty of localized states[5,29] $n_L$ close to MIT. Experimentally[49]

$$dG/dV \propto G(0) \propto n_s n_M \exp(-\kappa d)$$

is found in good agreement with our Eq. (2.5). The leakage current and $j_c$ degradation grows with $R_{bn}$ (Ref. 49) in line with our resonant tunnel model also. For the chemically different bismuthates with different $T_c$'s

$$G(0) \propto T_c$$

has been found, which may be explained by the $n_s$ dependence of Eq. (2.5).

## ACKNOWLEDGMENT

The discussions, support, and information of M. Beasley, A. Braginski, I. Boscovic, R. Gross, A. Junod, H. Küpfer, M. Lee, W. Schommers, J. Valles, and Y. Xu are gratefully acknowledged.

[1]See, e.g., K. C. Hass, in *Solid State Physics,* edited by H. Ehrenreich and D. Turnbull (Academic, New York, 1989), Vol. 42, p. 212; R. Byers and T. G. Shaw, *ibid.*, p. 135.

[2]See, e.g., L. H. Greene and B. G. Bagley, in *Physical Properties of High Temperature Superconductors II,* edited by D. M. Ginsberg (World Scientific, Singapore, 1991), p. 509.

[3]See J. Halbritter, in *Superconductivity and Applications,* edited by H. S. Kwok, Y. N. Kao, and D. T. Shaw (Plenum, New York, 1990), p. 351; J. Halbritter, P. Walk, H.-J. Mathes, B. Häuser, and H. Rogalla, Z. Phys. B **73**, 277 (1988).

[4]S. E. Babcock and D. C. Larbalestier, J. Mat. Res. **5**, 919 (1990); Appl. Phys. Lett. **55**, 393 (1989).

[5](a) M. V. Sadovskii, in *Proceedings of the International Workshop: Effect of Strong Disordering in HTSC, Zarechny, 1990* (U.S.S.R. Academy of Sciences, Moscow, 1990), p. 32; (b) R. C. Budhani, Sing-Mo H. Tzeng, and R. F. Bunshah, Phys. Rev. B **36**, 8873 (1987); A. Levy, J. P. Falck, M. A. Kastner, R. J. Birgeneau, A. T. Fiori, A. F. Hebbard, W. A. Gallagher, A. W. Kleinsasser, and A. C. Anderson, *ibid.* **46**, 520 (1992); (c) J. M. Valles, A. E. White, K. T. Short, R. C. Dynes, J. P. Gerno, A. F. J. Levi, M. Anzlawer, and K. Baldwin, *ibid.* **39**, 11 599 (1989).

[6]B. N. Goshchitskii, V. I. Voronin, S. A. Davydov, A. E. Karkin, and A. V. Mirmelstein, in *Proceedings of International Workshop: Effect of Strong Disordering in HTSC* [Ref. 5(a)], p. 14.

[7]G. S. Deutscher and P. Chaudhari, Phys. Rev. B **44**, 4664 (1991); P. G. de Gennes, Rev. Mod. Phys. **36**, 225 (1964).

[8]See, e.g., A. A. Golubov and M. Yu. Kupriyanov, Zh. Eksp. Teor. Fiz. **96**, 1420 (1989) [Sov. Phys. JETP **69**, 805 (1989)]; Phys. Lett. **154**, 181 (1991).

[9]T. Hasegewa, M. Nantoh, and K. Kitazawa, Jpn. J. Appl. Phys. **30**, L276 (1991).

[10]J. Lin, J. Wan, A. M. Goldman, Y. C. Chang, and P. Z. Jiang, Phys. Rev. Lett. **67**, 2195 (1991).

[11]Th. Becherer, J. Kowalewski, M. Schmitt, M. Huth, W. Assmus, and H. Adrian, Z. Phys. B **86**, 23 (1992).

[12]M. Lee, M. Naito, A. Kapitulnik, and M. R. Beasley, Solid State Commun. **70**, 449 (1989); M. Lee, D. Lew, C. B. Eom, T. H. Geballe, and M. R. Beasley, Appl. Phys. Lett. **57**, 1152 (1990).

[13]J. M. Valles, R. C. Dynes, A. M. Cucolo, M. Gurvitch, L. F. Schneemeyer, J. P. Garno, and J. V. Waszczak, Phys. Rev. B **44**, 11 986 (1991).

[14]R. Gross, P. Chaudhari, M. Kawesaki, and A. Gupta, Phys. Rev. B **42**, 10 735 (1990); R. Gross and B. Mayer, Physica C **180**, 235 (1991).

[15]S. E. Russek, Ph.D. thesis, Cornell University, 1990; S. E. Russek, D. K. Lathrop, B. H. Moeckly, R. A. Buhrman, D. H. Shin, and J. Silcox, Appl. Phys. Lett. **57**, 1155 (1990).

[16](a) R. Kleiner, F. Steinmeyer, G. Kunkel, and P. Müller, Phys. Rev. Lett. **68**, 2394 (1992); (private communication); (b) M. E. Klausmeier-Brown, G. F. Virshup, I. Boscovic, and J. N. Eckstein, Appl. Phys. Lett. **60**, 2806 (1992); R. Kleiner, Ph.D. thesis, TU München, 1992.

[17]E. L. Wolf, Principles of Electron Tunneling Spectroscopy (Oxford Science, London, 1989).

[18]J. Halbritter, Surf. Sci. **122**, 80 (1982); **153**, 80 (1982); J. Appl. Phys. **58**, 1320 (1985).

[19]P. Bradley, W. Ruby, D. Hebert, and T. van Duzer, J. Appl. Phys. **66**, 5872 (1989).

[20]M. S. Hybertsen, M. Schlüter, E. B. Stechel, and D. R. Jennison, Mat. Res. Soc. Symp. Proc. **168**, 19 (1992); W. Hanke, A. Muramatsu, and G. Dopf, Phys. Rev. Lett. **68**, 353 (1992).

[21]See, e.g., V. Z. Kresin and St. A. Wolf, Phys. Rev. B **41**, 4278 (1990).

[22]H. Claus, S. Yang, A. P. Paulikas, J. W. Downey, and B. W. Veal, Physica C **171C**, 205 (1990); H. Claus, M. Braun, A. Erb, K.-Röhberg, B. Runtsch, H. Wühl, G. Brändele, P. Schweib, G. Müller-Vogt, and H. v. Löhmeysen, *ibid.* **198C**,

42 (1992).
[23]M. Hawley, I. D. Raistrick, J. G. Beery, and R. J. Hulton, Science **251**, 1587 (1991); H. P. Lang, T. Frey, and H.-J. Güntherodt, Europhys. Lett. **15**, 667 (1991); H. P. Lang (private communication); W. Geyer (private communication).
[24]Y. Xu, A. Matsuda, and M. R. Beasley, Phys. Rev. B **42**, 1492 (1990).
[25]R. Berthe and J. Halbritter, Phys. Rev. B **43**, 6880 (1991).
[26]K. K. Likharev, IBM J. Res. Dev. **32**, 143 (1988).
[27]M. Naito and M. R. Beasley, Phys. Rev. B **35**, 2548 (1988); Tai Kai Ng and P. A. Lee, Phys. Rev. Lett. **61**, 1768 (1988).
[28]A. B. Kaiser, J. Phys. C **3**, 410 (1970).
[29]J. Halbritter, Solid State Commun. **18**, 1447 (1976); **34**, 675 (1989).
[30]J. A. Wilson, Physica C **182**, 1 (1991).
[31]B. J. van Wees, P. de Vries, P. Magnée, and T. M. Klapwijk, Phys. Rev. Lett. **69**, 510 (1992).
[32]I. K. Yanson, L. F. Rybalchenko, V. V. Fisun, N. L. Bobrov, M. A. Obolenskii, Yu. D. Tretyakov, A. R. Kaul, and I. E. Graboi, Fiz. Nizk. Temp. **15**, 803 (1989) [Sov. J. Low Temp. Phys. **15**, 445 (1989)].
[33]A. Junod, in *Physical Properties of High Temperature Superconductors II* (Ref. 2), p. 13.
[34](a) J. Halbritter, in *Proceedings of the Fifth Workshop on rf-Superconductivity, Hamburg, 1991,* edited by D. Proch (Deutsches Elektronen-Synchrotron DESY, Hamburg, 1992), p. 939; (b) J. Halbritter, J. Appl. Phys. **68**, 6315 (1990); **71**, 339 (1992).
[35]R. C. Dynes, J. P. Garno, G. B. Hertel, and T. P. Orlando, Phys. Rev. Lett. **53**, 2437 (1984).
[36]St. M. Anlage, B. W. Langley, G. Deutscher, J. Halbritter, and M. R. Beasley, Phys. Rev. B **44**, 9764 (1991).
[37]M. Kawasaki, P. Chaudhari, and A. Gupta, Phys. Rev. Lett. **68**, 1065 (1992).
[38]C. T. Rogers and R. A. Buhrman, in *Advances in Cyrogenic Engineering 32,* edited by R. P. Reed and A. F. Clerk (Plenum, New York, 1985), p. 489; IEEE Trans. Magn. **MAG-19**, 453 (1983).
[39]Y. Zhang, M. Mück, M. Bode, K. Herrmann, J. Schubert, W. Zander, A. Braginski, and C. Heiden, Appl. Phys. Lett. **60**, 2303 (1992).
[40]C. B. Eom, A. F. Marshall, Y. Suzuki, B. Boyer, R. F. W. Pease, and T. H. Geballe, Nature **353**, 544 (1991); Physica C **171**, 351 (1990).
[41]J. Halbritter (unpublished).
[42](a) M. E. Lopez-Morales, D. Rios-Jara, J. Tageiena, R. Escudero, S. L. Placa, A. Bezinge, V. Y. Lee, E. M. Engler, and P. M. Grand, Phys. Rev. B **41**, 6655 (1990). (b) Yunhui Xu and Weiyan Guan, Physica C **183**, 105 (1991).
[43]In-Sang Yang, A. G. Schrott, and C. C. Tsui, Phys. Rev. B **41**, 8921 (1990).
[44]Yu. M. Boguslavskij, J. Gao, A. J. H. M. Rijinders, D. Terpstra, G. J. Gerritsma, and H. Rogalla, Physica C **194**, 268 (1992).
[45]D. Lew, Y. Suzuki, C. B. Eom, M. Lee, J.-M. Triscome, T.-H. Geballe, and M. R. Beasley, Physica C **185-189**, 2553 (1991).
[46]Th. Zeiski, R. Sonntag, D. Hohlwein, N. H. Anderson, and T. Wolf, Nature **353**, 542 (1991); H. Lütgemeier (private communication).
[47]G. A. Baraff, E. O. Kane, and M. Schlüter, Phys. Rev. B **43**, 2648 (1991).
[48]J. W. P. Hsu, S. I. Park, G. S. Deutscher, and A. Kapitulnik, Phys. Rev. B **43**, 2648 (1991).
[49]F. Sharifi, A. Pargellis, and R. C. Dynes, Phys. Rev. Lett. **67**, 509 (1991); Physica C **185C**, 234 (1991).

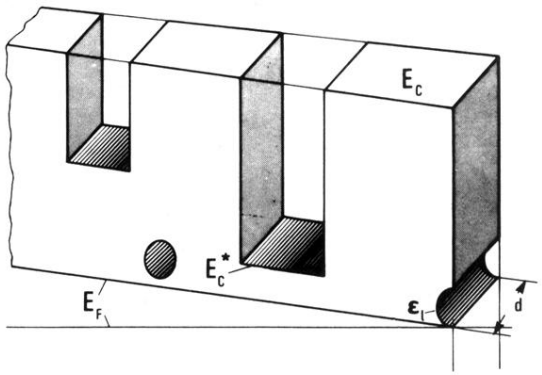


FIG. 2. Sketch of tunnel barriers with $E_c(r)$ the lower edge of the conduction band. Until now barriers $E_c(r)=E_c(x)$ being uniform along the electrodes have been treated, which cannot describe microcrystalline amorphous barriers like $Nb_2O_5$, $\alpha$Si or perturbed YBCO. The model depicted corresponds to $(E_c-E_F)=\Phi\simeq 1$ eV for crystallites, $(E_c^*-E_F)=\Phi^*\simeq 0.1-0.2$ eV for channels, and $(E_F-\epsilon_I)\geq 5$ meV for resonant tunneling via localized states symbolized as holes in the barrier. These three entities are the minimum set for the description of a "real" $Nb_2O_5$ barrier.[18] But it is obvious that actual barriers are not steplike and cannot be depicted so simply.